GEOELECTRICAL INVESTIGATION OF ROAD FAILURE ALONG MINNA-BIDA ROAD, NIGER STATE, NIGERIA

Supported by tetfund

A. A. Rafiu, T. A. Adesete, K.A Salako, A. A. Adetona, U. D. Alhassan, J. Shehu* and E. E. Udensi
Geophysics Department, Federal University of Technology, Minna, Niger State, Nigeria
*Corresponding author: jameelshehu@futminna.edu.ng

Received: January 15, 2020 **Accepted:** May 15, 2020

Abstract: The study is meant to reveal the horizontal and vertical geological discontinuities on the said road that has suffered repairs in the past. Probable zones of untimely failure along the road are then investigated by variation in resistivity. The resistivity values for profiles A, B, C, D and F range between 0.10 and 30.4 Ωm; indicating failed segments which are typical of fractured or fissured zone, as a result of clayey nature of the topsoil/sub-grade soil on which the road pavement is founded. The stable segment which is characterized by high ranging resistivity (16.4 – 4628 Ωm) shows no evidence of any major geologic feature such as fault and fractured zone that could have precipitated failure. The range of values characteristically places the regions in a basement complex area with the presence of clay-sandstone intercalation. The causes of road pavement failure on the studied road was found to be majorly as a result of a combination of clayey topsoil/sub grade soils, water-logged sands with characteristically low resistivity values and thin pavement unable to withstand pressure exerted on the road.

Keywords: Road failure, resistivity, pavement, top soil, failed segment

Introduction

Road failures have become a common problem in most parts of Nigeria. Major roads are known to fail shortly after construction. Because of the poor maintenance on the part of the government and due to the inadequate geophysical survey of the soil in the area, road failure occurs frequently in Nigeria. Rehabilitating the roads has become a financial burden on the Federal, State, and Local Governments (Adegok *et al*., 1980; Ajayi, 1987), hence the causes of road failures need to be identified and the means of ameliorating them sought. Some factors are responsible for road failures. These include geological, geomorphological, geotechnical, road usage, construction practices, and maintenance (Adegoke *et al*., 1980; Ajayi, 1987).

Field observations and laboratory experiments carried out by Adegoke *et al.* (1980), Mesida (1981), and Ajayi (1987) showed that usage or design construction problems are not only the primary cause of road failures, but it can equally occur due to inadequate knowledge of the characteristics and behavior of residual soils on which the road are built and non-recognition of the influence of geology and geomorphology during the design and construction phases.

Geophysics, for the past two decades, has proved quite relevant in highway site investigations (Nelson and Haigh, 1990), geophysical methods like electrical resistivity has been used in mapping subsurface geologic sequence and concealed geological structures (Olorunfemi *et al.*, 2000).

Materials and Methods

Geology of the study area

The geology of some of the area has been mapped by Truswell and Cope (Adeniyi, 1985). The rock types found here in the study area are believed to be part of the older granitic suite and mostly exposed along river channel were they appear in most case weathered. Base on relative grain size, the major rock types are; Porphyritic to coarse grained granite, North-south (N-S) trending quake and aplitic veins, the outcrops, medium to fine grained granite, The rocks are in some places broken into blunders, and show the effect of weathering in form of colour change, and loose rock fragment (Adeniyi, 1985).

Location of the study

The road investigated is in Minna, Niger State, Nigeria. The road serves as a link between Minna and Gidan kwano the major high way leading to Bida. This road also links Minna to southwestern part of part of Nigeria. It is delineated on latitude 9.294° 6̓ N and longitude 6.4563° 5̓ E as shown in Fig. 1.

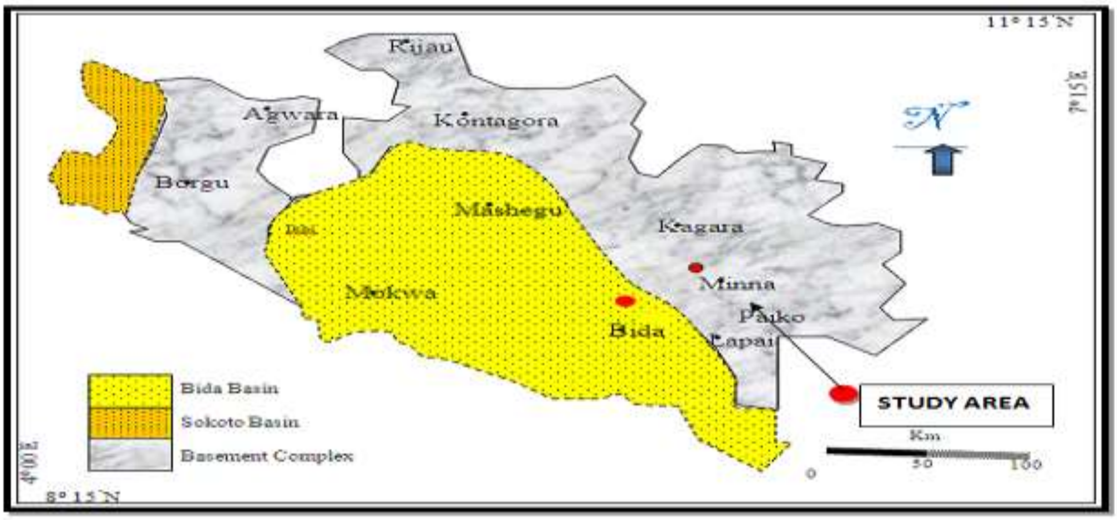

Fig. 1: Map showing the geology of Minna

Methods

Geophysical Survey Twenty VES points were measured using Schlumberger array with the aid of ABEM Terrameter SAS4000 and its accessories. Two profiles inside the dump comprise of sixteen VES and another four outside the dump to serve as control. A maximum current electrode separation of AB/2 of 80 m was used in this study. The apparent resistivity from the survey was processed by a computer software program called Winresist.

Results and Discussion

The results of the geoelectrical investigation from different profiles, which is different location of the failed sections along Minna-Bidaroad are presented below. The data were collected in order to automatically generate a one dimensional (1-D) and two dimensional (2-D) resistivity model for the subsurface which can be referred to as Electrical Image (Ebhohimen and Luke, 2014).

Figure 2I is the pseudo cross-section plot of apparent resistivity data for profile A with four VES points begins at coordinate 9.424° 5' Nand longitude 6.483° 4'E, end at coordinate 9.724° 9' N and longitude 5.262° 7'E. The blue regions occurs along the four VES points especially at VES 2, where the depth of the blue region is about 10 m and it occur at all the four VES points, which indicates very low resistivity value of 13.52 Ωm at the first layer, where the road is badly affected. VES 1 shows 2 layers (Fig. B), having a resistivity of 11.18 Ωm for the first layer with 2.79 m depth and thickness of 2.79 m, and 9244 Ωm for the second layer. VES 2 shows 2 layers; having a resistivity of 13.52 Ωm for the first layer with 9.889 mdepth and thickness of 9.889 m and 9244 Ωm for the second layer. VES 3 shows 2 layers; with a resistivity of 17.49 Ωm for the first layer with 4.276 m depth and thickness of 4.276 m and 9244 Ωm for the second layer. VES 4 shows 2 layers; having a resistivity of 11.18 Ωm for the first layer with 2.86 m depth and thickness of 2.86 m, and 9244 Ωm for the second layer. The topsoil is underlain by clay/sandy clay whose resistivity values range from 11.18 – 9244 Ωm. The bottom of the layer could not be delineated because of the short sounding spread. The failure along this segment of the road is apparently precipitated by differential settlement induced by the clayed substratum and this is line with the work of Michael *et al.* (2008).

Figure 3 is a Pseudo cross-section plot of apparent resistivity data for profile B, VES 1 shows 3 layers; the first layer having a resistivity of 3083 Ωm with 0.232 m depth and thickness of 0.232 m, 1.69 Ωm for the second layer with 0.697 m depth and thickness 0.697 m and 2090 Ωm for the third layer.VES 2 shows 3 layers; the first layer having a resistivity of 10.79 Ωm with 0.05 m depth and thickness of 0.05 m, 2239 Ωm for the second layer with 2.054 m depth and thickness 2.054 m and 11.22 Ωm for the third layer. VES 3 shows 2 layers; the first layer having a resistivity of 743 and 24.9 Ωm for the second layer at 0.586 m depth and thickness of 0.586 m respectively. VES 4 shows 3 layers; the first layer having a resistivity of 4815 Ωm with 0.437 m depth and thickness of 0.437 m, 1.25 Ωm for the second layer with 0.776 m depth and thickness of 1.21 m, 3900 Ωm for the third layer. VES 1 and VES 4 falls within the standard resistivity of clay ranging from 1 – 100 Ωm. The unstable segment of the road is characterized by low resistivity of the near surface materials and shallowness of the aquiferrous zone on which the road pavement was founded Adiat *et al.* (2009).

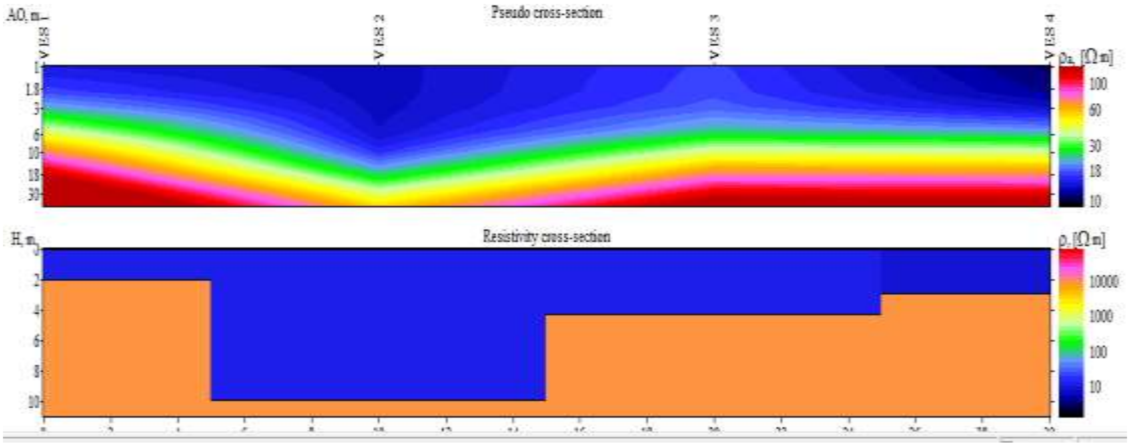

Fig. 2I: (a) Pseudo cross-section plot of apparent resistivity data profile A and (b) Resistivity cross section

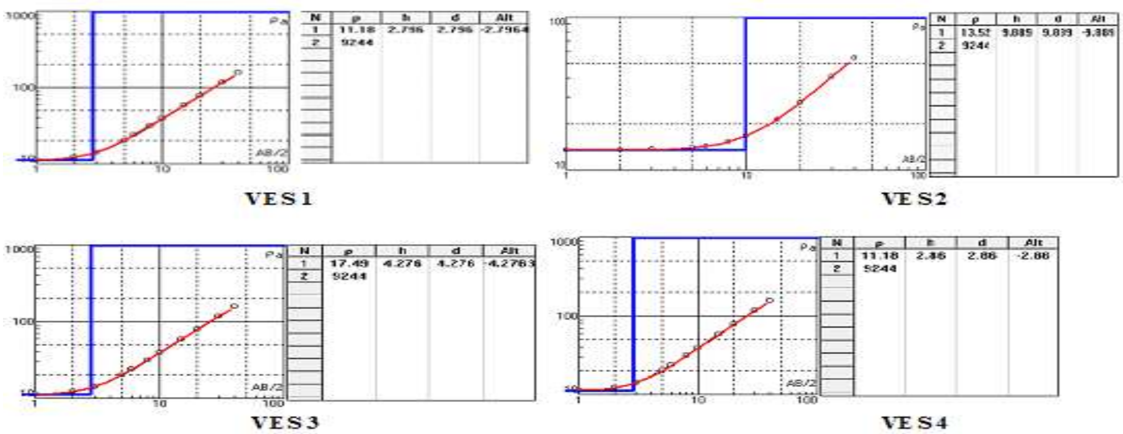

Fig. 2II: Resistivity pseudo section of profile A showing plots for VES 1, VES 2, VES 3 and VES 4

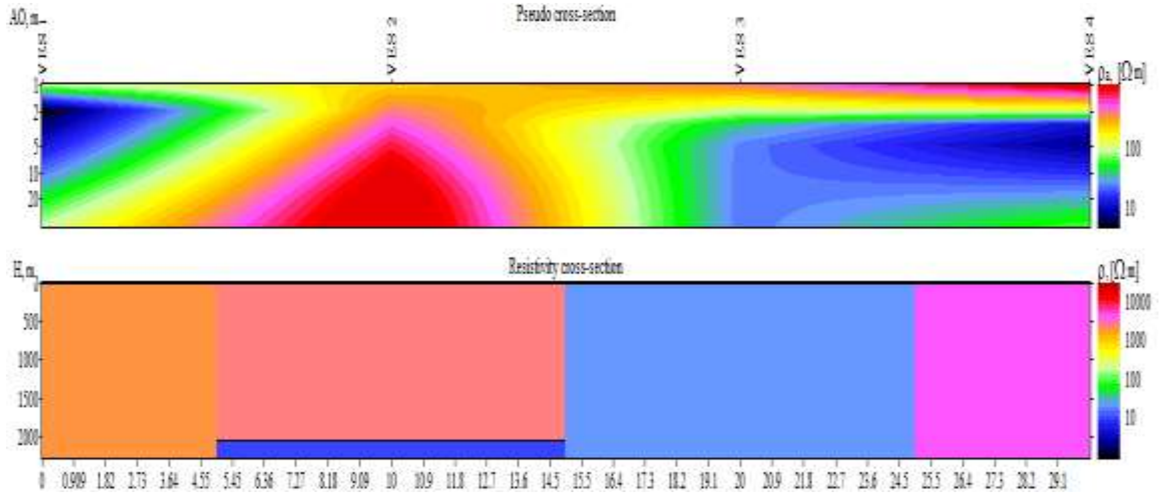

Fig. 3: (a) Pseudo cross-section plot of apparent resistivity data profile B and (b) Resistivity cross section

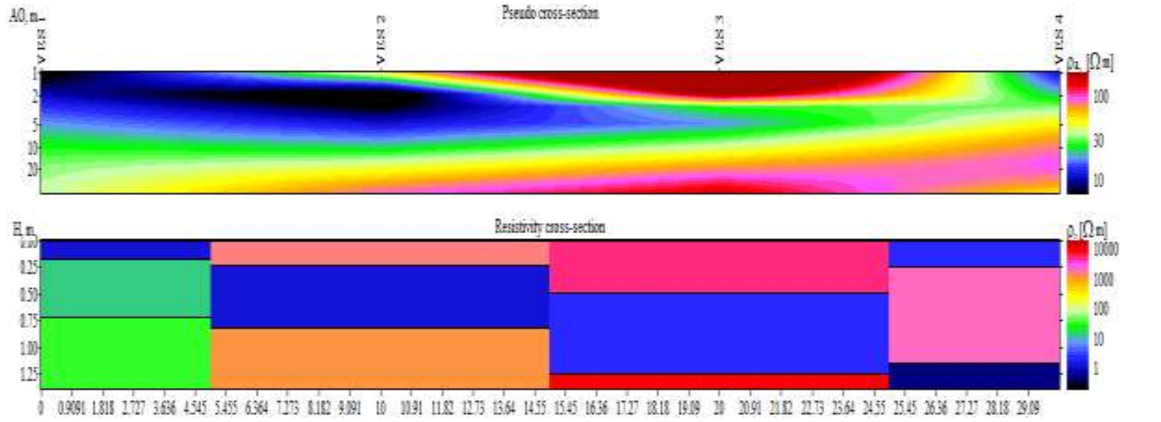

Fig. 4: (a) Pseudo cross-section plot of apparent resistivity data profile C and (b) Resistivity cross section

Figure 4 is a Pseudo cross-section plot of apparent resistivity data for profile C, VES 1 shows 3 layers; the first layer is made up of topsoil (clayey sand and sandy clay) which has resistivity of 1.588 Ωm with 0.1736 m depth and thickness of 0.1736 m, 38.62 Ωm for the second layer with the depth of 0.55 m and thickness of 0.7236 m, and 431.7 Ωm for the third layer. VES 2 shows 3 layers; the first layer having a resistivity of 1445 Ωm with 0.235 m depth and thickness of 0.235 m, 1.4 Ωm for the second layer with 0.584 m depth and thickness of 0.819 m and 1065 Ωm for the third layer.VES 3 showing 3 layers; the first layer having a resistivity of 5195 Ωm with 0.484 m depth and thickness of 0.484 m, 2.99 Ωm for the second layer with 1.25 m depth and thickness of 0.77 m and 9704 Ωm for the third layer.VES 4 shows 3 layers; the first layer having a resistivity of 2.521 Ωm with 0.2496 m depth and thickness of 0.2496 m, 220 Ωm for the second layer with 1.151 m depth and thickness of 0.9013 m and 0.6459 Ωm for the third layer. Average of 9704 Ωm at the third layer Ωm suggested a sedimentary environment while the low resistivity spectrum suggested areas of low permeability or clay intercalation. This is similar to the work of Ebhohimen and Luke (2014).

Figure 5 is a Pseudo cross-section plot of apparent resistivity data for profile D with four VES points. VES 1 shows 3 layers; the first layer having a resistivity of 836 Ωm with a depth 0.592 m and thickness of 0.592 m, 1.02 Ωm for the second layer with 1.43 m depth and thickness of 0.839 m and 1140 Ωm for the third layer. VES 2 showing 3 layers; the first layer having a resistivity of 2103 Ωm with 0.544 m depth and thickness of 0.544 m, 1.73 Ωm for the second layer with 1.58 m depth and thickness 1.73 m and 1379 Ωm for the third layer.VES 3 showing 3 layers; the first layer having a resistivity of 7235 Ωm with 0.404 m depth and thickness of 0.404 m, 1.12 Ωm for the second layer with 1.13 m depth and thickness of 0.725 m and 8542 Ωm for the third layer.VES 4 showing 3 layers; the first layer having a resistivity of 1.949 Ωm with 0.3162 m depth and thickness of 0.3162 m, 15216 Ωm for the second layer with 0.434 m depth and thickness of 0.1178 m and 2.371 Ωm for the third layer. The first layer of VES 1, VES 2 and VES 3 indicates a sedimentary rocks when compared with the standard resistivity of 8 – 4x10^3 Ωm and 10^2 – 2x10^8 Ωm for sandstone and quartzite respectively. While the second layer of VES points 1, 2 and 3 falls within the standard resistivity of clay ranging from 1 – 100 Ωm, and thus showing a weak zone along the region. This is line with the work of Momoh *et al.*, (2008).

Figure 6 is a Pseudo cross-section plot of Apparent Resistivity data for profile E with four VES points, VES 1 shows 3 layers; the first layer having a resistivity of 395.4 Ωm with 0.0879 m depth and the thickness of 0.0879 m, 77.43 Ωm for the second layer with 2.509 m depth and the thickness of 2.421 m and 59450 Ωm for the third layer. VES 2 shows 3 layers; the first layer having a resistivity of 78.68 Ωm with a depth of 2.488 m and the thickness of 2.488 m, 80950 Ωm for the second layer with a depth of 12.71 m and thickness of 10.22 m and 146791 Ωm for the third layer. VES 3 shows 3 layers; the first layer having a resistivity of 16.73 Ωm with a depth of 0.4291 m and the thickness of 0.4291 m, 3043 Ωm for the second layer with 1.442 m depth and the thickness of 1.013 m and 34.81 Ωm for the third layer. VES 4 shows 3 layers; the first layer having a resistivity of 7.308 Ωm with a depth of 0.3965 m and the thickness of 0.3965 m, 251.2 Ωm for the second layer with a depth of 22300 m and the thickness of 22300 m and 14302 Ωm for the third layer. The four VES points shows low resistivity at the first layer ranging between 16.73 – 78.68 Ωm which indicates fault zone and falls within the standard resistivity of clay ranging from 1 – 100 Ωm, respectively (Table 1); this indicates that the road is on soils and waters Nwokoma *et al.* (2015).

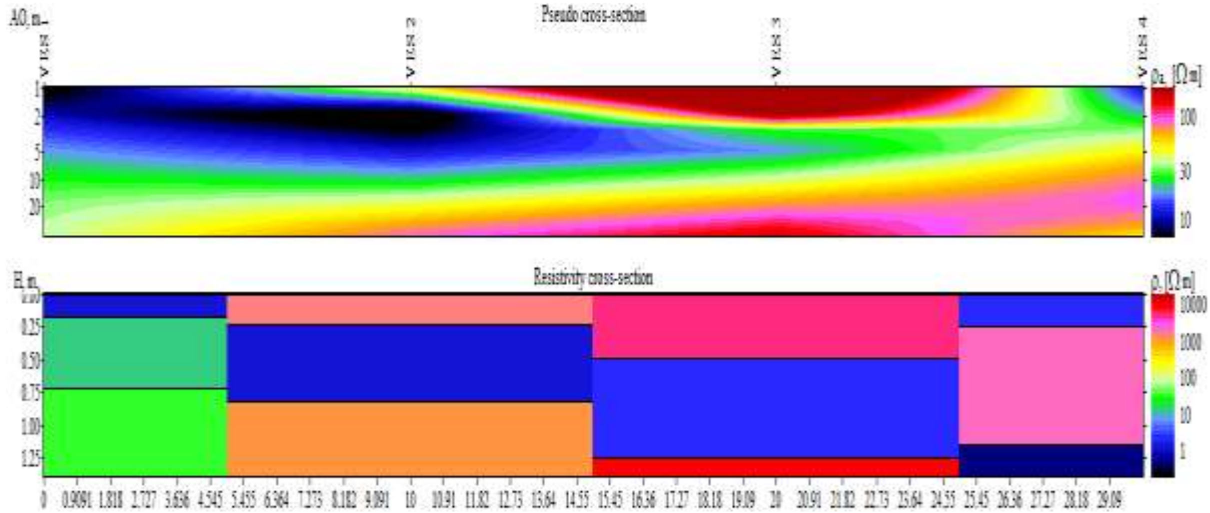

Fig. 5: (a) Pseudo cross-section plot of apparent resistivity data profile D and (b) Resistivity cross section

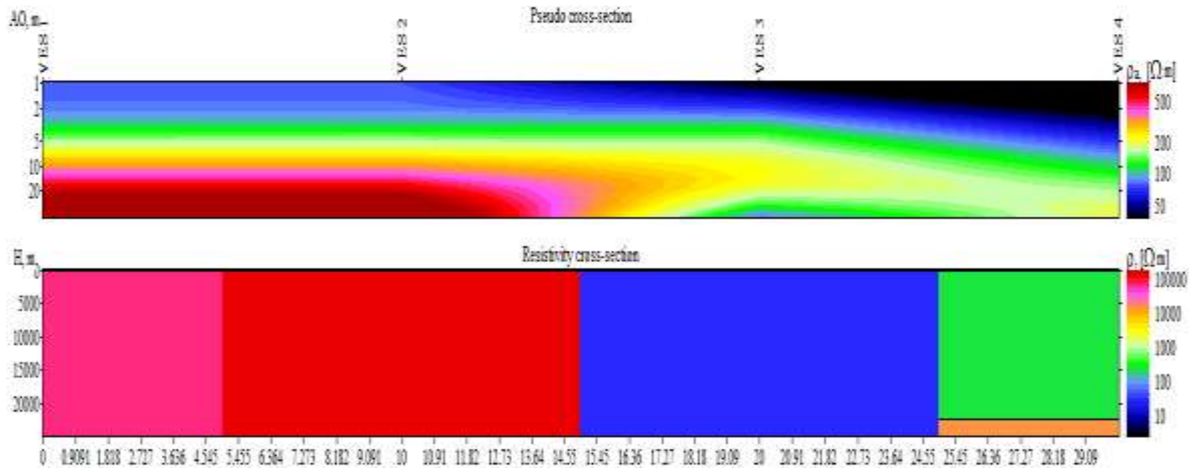

Fig. 6: (a) Pseudo cross-section plot of apparent resistivity data profile E and (b) Resistivity cross section

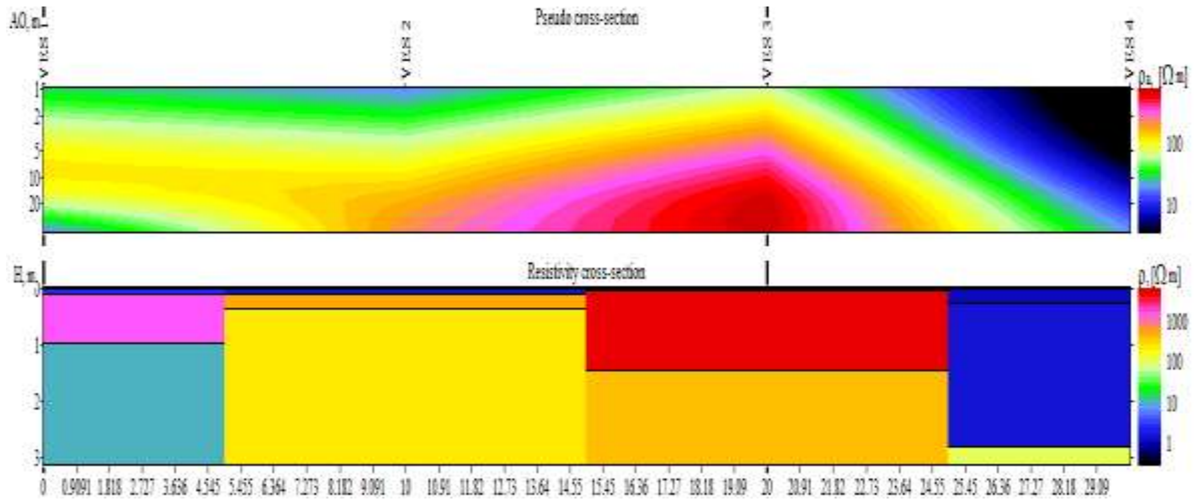

Figure 7: (a) Pseudo cross-section plot of apparent resistivity data profile F and (b) Resistivity cross section

Figure 7 is a Pseudo cross-section plot of apparent resistivity data for profile F with four VES points; begins at coordinate 9.429° 6' N and longitude 9.542° 8'E and ends at coordinate 9.974° 9' Nand longitude 9.527° 8'E. VES 1 shows 3 layers; the first layer having a resistivity of 3.396 Ωm with a depth of 0.1122 m and the thickness of 0.1122 m, 1334 Ωm for the second layer with a depth of 0.9716 m and the thickness of 0.8594 m and 12.23 Ωm for the third layer. VES 2 shows 3 layers; the first layer having a resistivity of 2.058 Ωm with 0.1039 m depth and the thickness of 0.1039 m, 488.1 Ωm for the second layer with a depth of 0.3687 m and the thickness of 0.2648 m and 261 Ωm for the third layer; the apparent resistivity at 0.3024 m ranges between 1.20983 to 4426.822 Ωm. VES 3 shows 3 layers; the first layer having a resistivity of 1.507 Ωm with 0.0230 m depth and the thickness of 0.0230 m, 11101 Ωm for the second layer with 1.442 m depth and the thickness of 1.419 m and 421.7 Ωm for the third layer. VES 4 shows 3 layers; the first layer having a resistivity of 1.397 Ωm with a depth of 0.2701 m and the thickness of 0.2701 m, 1.778 Ωm for the second layer with 2.811 m depth and thickness of 2.541 m and 115.2 Ωm for the third layer. Apart from the regions with few blue portions with low resistivity with indicates clay and water percolation. The vertical electrical sounding results indicates the occurrence of relatively thin topsoil of 0.1122 m composed of sandy-clay which is underlain by clay-shale formation to about 2.811 m depth, while the other portions with other colour shows competent zones with high resistivity as indicated above (Fatoba *et al.*, 2013).

Table 1: Typical resistivity values for different types of subsurface (Loke, 2000)

Materials	Resistivity (Ωm)	Rock Type
Granite	$5x10^3 – 10^6$	Igneous and metamorphic rock
Basalt	10^3 - 10^6	
Slate	$6x10^2 – 4x10^7$	
Marble	$10^2 – 2.5x10^8$	
Quartzite	$10^2 – 2x10^8$	Sedimentary rocks
Sandstone	$8 – 4x10^3$	
Shale	20 -$2x10^3$	
Limestone	50 -$4x10^2$	
Clay	1 – 100	Soils and Waters
Aluminum	10 – 800	
Groundwater (fresh)	0 – 100	
Sea water	0.2	

The 2-D dipole-dipole method was adopted to obtain the result in Fig. 8 and this was done by employing Wenner -2D modeling to produce two dimensional (2D) electrical imaging surveys which are widely used to map areas of moderately complex geology where conventional resistivity surveys and profiling may be inadequate (Table 1). Fig. 8 Shows measured apparent resistivity pseudosection where the blue portions indicate failed segments within the distances 7.5 - 47.5 m with low resistivity between 4.24 to 20.3 Ωm with the depth of 2.79 m and thickness of 2.79 m. The sub-grade soil which is the weathered layer beneath the topsoil is generally clayey within the distance between 20.5-120.5 m with resistivity range of between 4.24 and 20.3 Ωm. The mean thickness is 10.4 m. Fig. 8(b) shows calculated apparent resistivity pseudosection where the blue portions indicate failed segments within the distances 7.5 - 49.5 m with low resistivity between 4.24 to 20.3 Ωm with 7.5 m depth and thickness of 9.889 m. Fig. 8(c) shows computer interpreted iterated inverse model resistivity showing where the blue portions indicate failed segments within the distances 70.0 – 85.0 m with the depth and thickness of 4.276 and 120 – 135 m with the depth of 13.4 m and thickness of 13.4 m having low resistivity between 4.24 to 20.3 Ωm. The stable segment is characterized by high resistivity lateritic subsoil in the upper 10-23 m, 45-68 m and 87 – 120 m. The composition of the topsoil is typical of sandy clay/clayey sand (Momoh *et al.*, 2008).

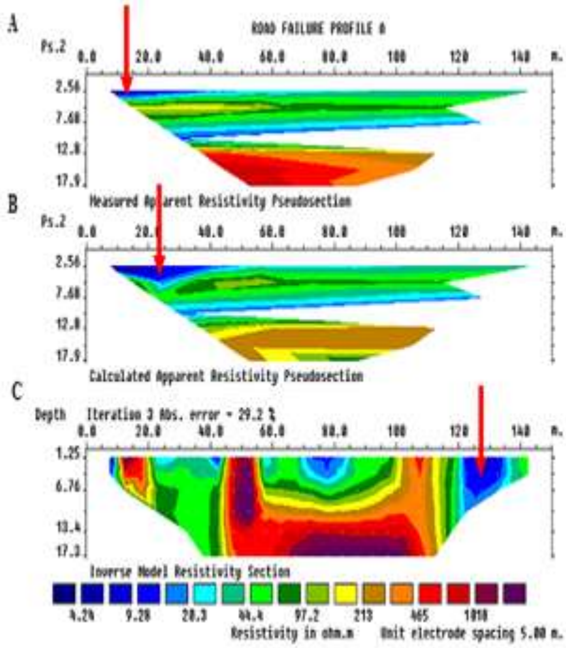

Fig. 8: Pseudosection plot shows apparent resistivity data of profile A showing the stratified layers for the Minna-Bida road. (a) Measured apparent resistivity pseudosection (b) Calculated apparent resistivity pseudosection (c) Inverse model resistivity section
The arrow indicates the affected portions of the road.

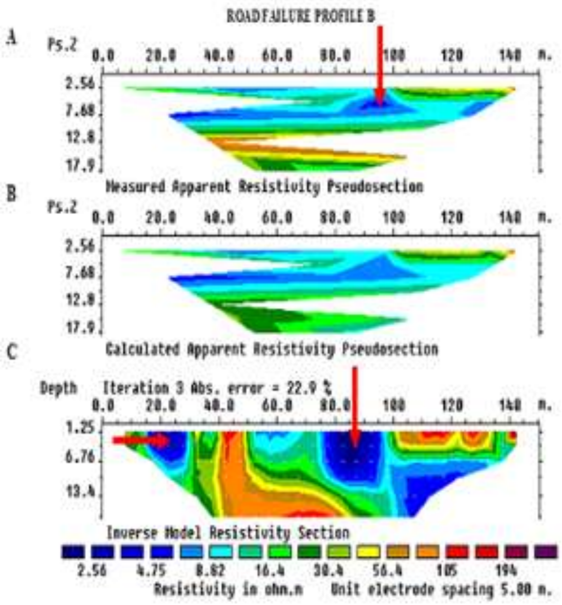

Fig. 9: Pseudosection plot of apparent resistivity data of profile B showing the stratified layers for the Minna-Bida road. (a) Measured apparent resistivity pseudosection (b) Calculated apparent resistivity pseudosection (c) Inverse model resistivity section
The arrow indicates the affected portions of the road.

Figure 9(a) is the measured apparent resistivity pseudosection where the blue portions indicate failed segments between the distances 20.0 – 100.0 m with low resistivity between 2.56 to 8.82 Ωm. The corresponding thicknesses of this layer range between 2.5 and 12.5 m with a mean value of 7.53 m for the first layer and 12.8 m for the second layer. Fig. 9(b) shows calculated apparent resistivity pseudosection where the blue portions indicate failed segments between the distances 20.4 – 140 m with low resistivity between 2.56 to 8.82 Ωm. The corresponding thicknesses of this layer range between 2.56 and 12.5 m with a mean value of 7.53 m. Fig. 9(c) shows computer interpreted iterated inverse model resistivity showing where the blue portions indicates failed segments between the distances 20.0 – 30.0 m and between 50.0 – 135.0 m, the corresponding thicknesses of this layer range between 1.25 and 16 m with a mean value of 8.6 m, with low resistivity between 2.56 to 8.82 Ωm. The blue portion along 120 – 140 m with about a depth of 13.4 m shows a very low resistivity of about 4.24 Ωm which indicates very high clay content and a bad portion of the road. The presence of clay soil in foundation materials is capable of causing swelling and brokerage of road surfaces when in contact with moisture during wet season. The portion of the road from Fig. 8(c) at the distance from 30 to 50 m and 100 to 140 m shows no evidence of any major geologic feature such as fault and fractured zone that could have precipitated failure. The overall results showed that poor foundation materials and poor Engineering construction have affected the rate of failure of the road especially the most affected portion that have gone through several rehabilitations (Ifabiyi *et al.*, 2013).

Conclusions

Based on the results of the geoelectrical investigation of road failure along Minna-Bida road, the following conclusions are drawn.

i. Clayey topsoil/sub-grade soils have tendency of absorbing water which makes them swell and collapse under imposed wheel load stress which subsequently lead to road failure, as observed at failed segment especially along profiles A, B, C, D and F.
ii. Presence of near surface linear features such as faults, fractured zones, fissures and joints contributes to the failed segment of the road.
iii. The range of resistivity values on profiles A (4.24 - 1018 Ωm), D (227 - 4628 Ωm), E (126 - 1978 Ωm) and F (2.52 - 1285 Ωm) characteristically placed the regions in a basement complex area with the presence of clay-sandstone intercalation which is not a water bearing zone.
iv. The range of resistivity values on profiles B (2.56 - 194 Ωm) and C (1.01 - 127 Ωm) characteristically placed the regions in a clay soil which has the tendency of absorbing water and makes it swell and collapse under imposed wheel load stress.

Conflict of Interest

Authors have declared that there is no conflict of interest reported in this work

References

Adegoke OF, Anthony WC & Agada OA 1980. Geotechnical characteristics of some residual soils and their implications on road design in Nigeria. *Technical Lecture:* Lagos, Nigeria. 1 – 16.

Adeniyi JO 1985. Geophysical Investigation of the central part of Niger State of Nigeria. Ph.D Thesis, University of Wisconsin, Madison, USA.

Adiat KAN, Adelusi AO & Amigun JO 2009. Integration of surface electrical prospecting methods for fracture detection in precambrian basement rocks of Iwaraja area Southwestern Nigeria. *Ozean J. Appl. Sci.*, 2(3): 1943 – 2429.

Ajayi LA 1987. Thought on road failures in Nigeria. *The Nig. Engr.*, 22(1): 10 – 17.

Ebhohimen V & Luke M 2014. Geophysical investigation of road failure in Opoji Enugu State, Nigeria. *Int. J. Scientific & Engr. Res*., 5(1).

Fatoba JO & Salami BM 2004. Geophysical investigation of ground subsidence: A case study of a beverage factory site in Edo State, Nigeria. *Global J. Geol. Sci.* 2(1): 153-159.

Ifabiyi IP & Kekere AA 2013. Geotechnical investigation of road failure along Ilorin: Ajase – Ipo Road Kwara State, Nigeria. *J. Envt. and Earth Sci.*

Loke MH 2000. Tutorial: 2-D and 3-D electrical Imaging Surveys Copyright (1996 - 2004).

Mesida EA 1981. Laterites on the highways – Understanding soil behaviour. *West Afr. Technical Rev*., 112 – 118.

Michael IO, Martins OO & John SO 2008. Geophysical investigation of road failures in the basement complex areas of Akure, Ondo State, Southwest Nigeria. *Res. J. Appl. Sci.*, 3(2): 103-112.

Momoh LO, Akintorinwa O & Olorunfemi, MO 2008. Geophysical investigation of highway failure - A case study from the basement complex terrain of south-western Nigeria. *J. Appl. Sci. Resistivity*, 4(6): 637-648.

Mubarak AF & Samuel OO 2015. Geophysical and geotechnical characterization of newly constructed Abadina-Ajibode road, University of Ibadan, Ibadan. *J. Multidisc. Engr. Sci. and Techn.* (JMEST), 2(1): 3159-0040.

Nelson RG & Haigh JH 1990. Geophysical investigation of lateritic terrain. *Geotechnical and Environmental Geophysics*. Ward SH (Ed), (Geotechnical), SEG. *Tulsia*, 2: 133 – 154.

Nwokoma EU, Chukwu GU & Amos-Uhegbu C 2015. Geoelectrical investigation of soils as foundation materials in Umudike Area, Southeastern Nigeria. *Physical Sci. Int. J.*, 6(2): 82–95.